Fuel 413 (2026) 138317

Contents lists available at ScienceDirect

Fuel

journal homepage: www.elsevier.com/locate/fuel

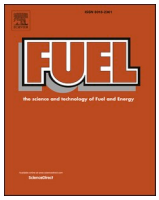

Full Length Article

The effect of CO2 and increased initial pressure on hydrothermal liquefaction for the production of high value fatty acids

D. Liakos [a], Maria Iosifidou [b], S. Vakalis [a,b,*]

[a] Department of Process Analysis and Plant Design, School of Chemical Engineering, National Technical School of Athens, 9 Heroon Polytechniou, GR-15780 Athens, Greece

[b] Energy Management Laboratory, Department of Environment, University of the Aegean, University Hill, 81100 Mytilene, Greece

ARTICLE INFO

Keywords:
Biocrude
Carboxylation
Hydrothermal
Plasma Gas Chromatography

ABSTRACT

Hydrothermal liquefaction (HTL) of waste biomasses has been widely studied, yet the influence of the reaction atmosphere on carboxylation chemistry is often overlooked. In this study, HTL of anise (*Pimpinella anisum* L.) waste was performed at 310, 350 and 390 °C solely with air (no added pressure), under N_2 with and without increased initial pressure, solely with CO_2, and with combined N_2/CO_2 and increased pressure. The aim was to assess how total pressure and gas/ atmosphere composition affect product distribution and high-value compound formation. Dissolved CO_2 was found to acidify the aqueous phase and participate in carboxylation reactions that convert hydrolysis intermediates into volatile fatty acids (VFAs), as measured via a GC-BID in the form of fatty-acid methyl esters (FAMEs). Chemical oxygen demand (COD) in the aqueous phase increased from 10,000 to 30000 mg/ L and was consistently higher under CO_2. Hydrochar higher heating value peaked at approximately 35 MJ/ kg at 350 °C and declined at 390 °C. CO_2-rich runs exhibited an order-of-magnitude increase in VFA production, with acetic-acid concentrations up to 2 g/ L. FAMEs formation increased with temperature; at 390 °C the combined N_2/ CO_2 system produced methyl hexanoate concentrations of approx. 13 g/ L and methyl octanoate 11.9 g/ L, more than threefold higher than in single-gas or non-pressurized runs. One-way ANOVA revealed that pressure significantly influenced VFA and FAME yields at 310–350 °C but this effect diminished at 390 °C. These results highlight the importance of optimizing both gas atmosphere and pressure in HTL processes and demonstrate that reactive CO_2 atmospheres can drive carboxylation pathways leading to higher yields of valuable fatty acids.

1. Introduction

Population growth acts as a key driver leading to the intensification of agriculture and food production, forming a large volume of organic waste, most of which is deposited in landfills [1]. According to Aierzhati et al. [2] one-third of food produced worldwide for human consumption is either wasted or lost. This ratio is equivalent to 1.3 billion tons of food per year [3]. Of the total volume of food waste, 54% is from food lost in the stages of production, post-collection handling and storage, and 46% is from food from the stages of processing, distribution and consumption stages [4]. Solid municipal waste is estimated to increase significantly due to rapid and rapid urbanization, industrialization and population growth and is expected to reach 9.5 billion by 2050. In this food waste makes up 25–70% of municipal solid waste [5]. The amount of food waste resulting from all the above stages and ending up in landfills causes significant pollution through their nutrients and greenhouse gas emissions [1]. More specifically, gases such as methane (CH_4) and carbon dioxide (CO_2) as well as leachate of these organic wastes pollute both soil and groundwater [2]. Methane released from rotting food waste in landfills is a gas 20 times more potent than carbon dioxide in rendering climate change over a 100-year time frame. Landfills are the third largest source of methane emissions in the United States [6]. In general, both food production and food waste indirectly contribute to a wide range of environmental impacts at all stages, i.e. from the stage of food production, storage, and transport to the stage of waste management [7]. It is important to promote and develop new waste to energy projects and facilities both for the management of the volume of organic waste and for the creation of value-added recovery systems [1]. This

* Corresponding author at: Department of Process Analysis and Plant Design, School of Chemical Engineering, National Technical School of Athens, 9 Heroon Polytechniou, GR-15780 Athens, Greece.
E-mail address: svakalis@chemeng.ntua.gr (S. Vakalis).

https://doi.org/10.1016/j.fuel.2026.138317
Received 30 July 2025; Received in revised form 24 December 2025; Accepted 6 January 2026
Available online 8 January 2026

organic waste is a carbon supply tank that can be used to generate energy [8]. More specifically, raw materials with high moisture content such as food waste have an advantageous position in the technology of hydrothermal liquefaction [9].

Food waste is defined as food the production of which was intended for human consumption but was discarded or not consumed by humans themselves. Edible food that is deliberately discarded is also in this category [10]. The anise waste that was used in this study as raw material belongs to the category of food waste. More analytically, the plant *Pimpinella anisum* L., which is popularly known by the common name anise, belongs to the family *Umbelliferae* and is a native plant of the Middle East [11]. The seeds of anise are rich in fatty oils, proteins, carbohydrates, cellulose fiber and anethole [12]. Anethole and especially its oils give the characteristic taste for which anise stands out [13]. In addition, anethole has an important role in the manufacture of alcoholic beverages using anise, as it is the main volatile compound [14], which determines the sweet taste that anise imparts to drinks [15]. In the Mediterranean it is common to aromatize alcoholic beverages with anise and in Greece this is the case with "ouzo" [11]. Ouzo is the most popular distilled alcoholic in Greece and is produced on the island of Lesvos [16]. In addition, anise imparts its special flavor to a wide range of alcoholic beverages worldwide such as Turkish raki, pastis in France, anesone in Spain, Sambuca in Italy, Zebib in Egypt, Arak in Syria and zivania in Cyprus [17]. It is worth noting that the oils of anise have extensive use in a variety of fields such as medicine, pharmacy due to its antimicrobial, antiparasitic, antioxidant properties while at the same time in cosmetics and food industries using the natural color of anise as well as aromatic-spice [17,18]. Therefore, the widespread use of anise for the production of a variety of products by spirits companies and industry, as well as the high moisture levels of waste anise during the production of ouzo and similar drinks after distillation, make it a raw material suitable for hydrothermal liquefaction [19].

The technology of hydrothermal treatment and by extension hydrothermal liquefaction belongs to the category of thermochemical processes [20]. This process converts low-quality biomass into high-quality biofuels and high-value added bio-products [21]. Hydrothermal liquefaction occurs under high pressure and temperature conditions, in the presence of the aqueous element, forming an environment with high reactivity [22]. This thermochemical process takes place in a temperature range of 280–370 °C and a pressure of 10–25 MPa. Under these conditions water acquires exotic properties by reducing its dielectric constant and is an important reactive medium and catalyst in the process starting directly the breakdown and conversion of biomass [23]. As raw material can be used organic waste that has high amount of moisture, organic waste with high organic content as well as high lignin content. Materials which cannot be further processed and are a source of carbon and by extension energy [24]. Compared to other waste to energy technologies, hydrothermal liquefaction offers energy savings as no drying preparations are required to process biomass [25]. The main products of hydrothermal liquefaction are the following: 1. hydrochar is a solid product rich in carbon and with similar properties to charcoal 2. Bio-crude oil is the main liquid fuel product of hydrothermal liquefaction. It is a viscous dark brown oil containing a large number of hydrocarbons, aromatic compounds and many oxygenated compounds [26]. The gaseous products of the process mainly include CO_2, and smaller fractions of CO, H_2 and CH_4. These products are derived from reactions of decarboxylation and cracking of organic compounds that take place during hydrothermal liquefaction [27]. As reported by Vardon et al. [28] bio-crude consists of a range of chemical compounds determined by the type of biomass. In the components of bio-crude occur straight and branched aliphatic compounds, aromatic and phenolic derivatives, esters, carboxylic acids and nitrogenous ring structures [28]. Similarly with Shanmugan et al. [29] regarding a bio-crude oil study by algal biomass, is characterized as a complex mixture of oxygenated hydrocarbons and nitrogenous compounds. More specifically, aromatics, short-chain carboxylic acids, ketones, phenolic compounds, sugars and furan derivatives. It is also stated that the concentration of the above components depends on the type of biomass [29]. In a more general description, due to high temperature conditions the dielectric constant of water [30] decreases and thus appears to behave as a non-polar organic solvent [31]. This change contributes to the breakdown of macromolecules thus starting the processes for the conversion of biomass [32].

At this point it is worth giving a more extensive reference and description of the reactions that take place to the formation of the bio-crude oil. The first stage of reactions begins with hydrolysis. Through hydrolysis, biomass macromolecules are degraded into smaller molecules, such as proteins hydrolyzed into amino acids, lipids into glycerol and long-chain fatty acids, carbohydrates into reducing sugars, and lignocelluloses into glucose and alcohol monomers [33]. The majority of produced molecules resulting from hydrolysis don't show stability under hydrothermal treatment conditions, being chemically unstable [34]. This makes the molecules susceptible to reactions mainly decarboxylation, dehydration, isomerization, etc [35]. More specifically, in the next stage, reactions of decarboxylation, deamination, decomposition and polymerization take place, and form carboxylic acids, alkanes, olefins, ketones and gas compounds with nitrogen respectively. Then, decomposition and dehydration reactions of some intermediates follow, to produce stable molecules, unchanged in each phase [33]. In subcritical water, monosaccharides are highly reactive and decompose through condensations producing aldehydes, ketones, carboxylic acids and by dehydration forming furans and phenolic compounds [36]. On the other hand, aldehydes and ketones from the degradation of cellulose can form through condensation and dehydration aromatic compounds [23]. Amino acids, present in hydrothermal conditions, follow two reaction pathways, decarboxylation and deamination to produce organic acids (carboxylic acids), ammonia and carbon dioxide [37]. These two important reactions for the production of carboxylic acids, structural components of biocrude, take place simultaneously and there is competitive behavior under hydrothermal conditions [38]. This relationship is determined by the pH of the reaction medium, the location of the amino group and the alkyl side chain, factors that affect the velocity constants of the two reactions [39]. Long-chain fatty acids exhibit stability in compressed water and under hydrothermal conditions, partially degrade, further to long-chain hydrocarbons having excellent fuel properties. They degrade through decarboxylation reactions, favored by alkaline pH [23]. According to Watanabe et al. [40], stearic acid ($C_{17}H_{35}COOH$) decomposed into hydrocarbon in supercritical conditions and specifically at 400 °C, 25 MPa pressure and 30 min residence time [40]. This stability of fatty acids results in bio-crude oil under subcritical conditions, to have a high content of fatty acids [23]. Biller and Roth [41], point out similarly that the most basic part of bio-crude consists of fatty acids. In particular, the heaviest fatty acids derived from carboxylic groups [42]. In addition, Vo et al. [43] report after research that lipids and proteins are the main contributors to the formation of bio-crude oil. Carbon dioxide plays an important role in the production processes of bio-crude oil, which directly influences and acts as a catalyst in the production of the most basic components of bio-crude oil. As reported, by Rogalinski et al. [44], the addition of CO_2 contributed to the greater efficiency of amino acids formation at the stage of hydrolysis. Although HTL is widely studied for biomass conversion, the specific role of CO_2 in the process and its impact on product composition remain insufficiently explored. Limited research has examined how CO_2 influences reaction pathways, particularly in the formation and quality of VFAs and fatty acids (FAs), which are key biofuel precursors. Understanding CO_2's effect on their yield and selectivity is crucial for optimizing HTL conditions and improving bio-oil quality, highlighting the need for further investigation in this area.

The present study aims to explore the management and valorization of anise waste through the process of HTL, with the ultimate goal of converting this waste into biofuels and value-added bioproducts. Specifically, the study seeks to assess the operational performance of the

HTL process under varying pressure conditions by introducing different gaseous environments at the initial stage of the reaction. The gases utilized in the study include carbon dioxide, nitrogen, and a combination of both, with a particular focus on their influence on the physicochemical properties and yield of the resulting products. A key aspect of the investigation is to elucidate the role of CO_2 in the HTL process and its impact on the production efficiency and compositional characteristics of the bio-derived products. Special emphasis is placed on the formation and distribution of VFAs and FAMEs, as these compounds are crucial indicators of biofuel potential and overall process efficiency. A comprehensive series of analytical techniques is employed to evaluate the quality and composition of the obtained bio-oil, providing insights into the mechanisms by which the presence of CO_2 influences the reaction pathways and the physicochemical transformation of biomass. By systematically examining the effect of different pressure conditions on the HTL process, this study aims to contribute to the optimization of biofuel production from anise waste, advancing sustainable waste-to-energy strategies and enhancing the applicability of hydrothermal technologies for biomass conversion.

2. Material and Methods

2.1. Experimental Design and analytical Methods

The raw material for this study was anise waste. This waste was taken from a local distillery on the island of Lesvos. In particular, it was used as an additional ingredient of ouzo during its distillation in order to give flavor and aroma to the alcoholic beverage. This waste after distillation was collected and calculated the percentage of moisture and Total Solids (TS) after drying at 105 °C for 24 h and then with additional heating at 550 °C for 2 h the Volatile Solids (VS) were measured. Anise waste was the raw material in hydrothermal liquefaction experiments carried out in a hydrothermal reactor.

The experiments of hydrothermal liquefaction of anise waste took place at a Parr 4577A hydrothermal reactor, with a capacity of 1 L. The experiments were carried out at three different temperatures of 310 °C, 350 °C and 390 °C and the overall conditions are presented in Table 1. Each temperature included four individual experiments. These experiments for each temperature were: hydrothermal liquefaction without adding pressure at the beginning of the process, adding 10 bar pressure with nitrogen gas, adding 9 bar nitrogen gas pressure and 1 bar carbon dioxide gas pressure and finally an experiment with adding at the beginning of the hydrothermal process 1 bar carbon dioxide gas pressure. In other words, at each temperature, four different versions of pressure addition were performed. The process began with adding the amount of waste to the hydrothermal reactor. At 310 °C the amount of waste was 200 gr, at 350 °C, 100 gr of anise waste was placed in the reactor, while at 390 °C, 50 gr of the raw material was added. Then, the reactor was sealed and the oxygen from inside was cleared out with the addition of 10 bars of nitrogen gas, thus creating anoxic conditions. The process of removing oxygen was carried out in all the experiments. Then followed the addition of pressure with the gases and the versions mentioned above. At all temperature conditions the residence time of the anise waste was 2 h as shown in the table.

Table 1
Hydrothermal liquefaction conditions.

Sample	Description	m (gr)	T (°C)	P (bar)
S310NoP	No Pressure	200	310	100,7
S310N_2P	10 bar N_2 Pressure	200	310	125
S310N_2CO_2P	1 bar CO_2 & 9 bar N_2 Pressure	200	310	124
S310CO_2P	1 bar CO_2 Pressure	200	310	104,4
S350NoP	No Pressure	100	350	120,9
S350N_2P	10 bar N_2 Pressure	100	350	146,6
S350N_2CO_2P	1 bar CO_2 & 9 bar N_2 Pressure	100	350	147,8
S350CO_2P	1 bar CO_2 Pressure	100	350	128,9
S390NoP	No Pressure	50	390	77,2
S390N_2P	10 bar N_2 Pressure	50	390	112,3
S390N_2CO_2P	1 bar CO_2 & 9 bar N_2 Pressure	50	390	112,2
S390CO_2P	1 bar CO_2 Pressure	50	390	92,8

With the end of hydrothermal liquefaction started the cooling process of the reactor. During the cooling of the reactor, the collection of gaseous products was carried out and this is because with the drop in temperature there was a decrease in pressure which helped in the controlled exit of gases from the reactor. During the collection, the gas was passed through a distillation column in order to liquefy the heavy tar fractions and then passed through a solvent trap to be purified from more volatile tar fractions. Finally, the gas was stored in Tedlar bags with a capacity of 1 L. Upon completion of cooling, the reactor was opened, and the liquid and solid products were collected. Initially, they were separated by centrifugation and then further separated by Büchner funnel filtering. Then, the biocrude was separated from the aqueous phase by a separating funnel and the use of dichloromethane. Consequently, through a rotary evaporator, the biocrude was separated from the organic solvent and the products were weighed. The following are the equations used to calculate mass yield %, the acronym G.A.L concerns gases, aqueous phase and losses:

$$Hydrocharyield(\%) = \frac{massofhydrochar(gr)}{massoftotalanise(gr)} \times 100 \quad (1)$$

$$Biocrudeyield(\%) = \frac{massofbiocrude(gr)}{massoftotalanise(gr)} \times 100 \quad (2)$$

$$massofG.A.L(gr) = massoftotalanise(gr) - (massofhydrochar(gr) + massofbiocrude(gr) \quad (3)$$

$$G.A.Lyield(\%) = \frac{massofG.A.L(gr)}{massoftotalanise(gr)} \times 100 \quad (4)$$

With the end of hydrothermal liquefaction, the collection of products, their separation and weighing followed a series of qualitative analyses mainly on the liquid and solid parts of the products. More specifically, in order the analyses that followed are as follows: pH, conductivity, COD, total phenols, High Heating Value (HHV), VFAs, FAMEs and gaseous products as described in Liakos et al. [45]. The values of pH and conductivity were measured via the Consort C932 device. Their calculation was aimed at understanding and studying the conditions and processes that took place for the production of biofuels and bioproducts. To measure them, calibration was done for more accurate results such as Sklavos et al. [46].

Before beginning the process of measuring of COD the samples were filtered with 0.45 μm filters. After that, the calculation of COD started with dilution of all samples. More specifically, for the samples of 310 °C the dilution with water was 1/200, while the samples of 350 °C and 390 °C the dilution was 1/100. Then a mixture was prepared including 2.8 ml Silver Sulfate (Ag_2SO_3), 1.2 ml potassium dichromate ($K_2Cr_2O_7$) and 2 ml diluted sample according to the methodology of APHA, 1998. This mixture was made for all samples. Afterwards, measurement of COD concentration followed on a Hach DR3900 spectrophotometer [47]. Regarding the measurement of the concentration of total phenols, it started by filtering with a 0.45 μm filter and then diluting the samples with water. The S310NoP and S310N_2P samples were diluted 1/200. The S390NoP sample was diluted 1/500 and the residual samples were diluted 1/250. Then followed the preparation of a mixture of 10 ml diluted sample, 0.5 ml Folin-Ciocalteu Reagent (FCR) and 1.5 ml Sodium Carbonate (Na_2CO_3) [48]. This procedure was carried out for all samples. The determination of the concentration of total phenols was carried out on a Hach DR3900 spectrophotometer. The HHV measured for both hydrochar and bio-crude oil. As for hydrochar, the process for the measurement of HHV began by extracting from its pores some oily phases through Soxhlet extractor with the use of isopropanol. Then the Hydrochar dried at 105 °C for 24 h to remove the organic solvent and

moisture. After that the dried hydrochar and specifically an amount of 0.3 gr was ready for the calculation of HHV in a Parr 6400 Bomb Calorimeter [49].

Finding the concentration of VFAs began with a pre-treatment extraction from bio-crude oil. The process began by filtering the liquid (bio-crude oil) through Buchner funnel filter flask to avoid possibly solids. Then, they were placed in a tube, 3 ml of sample and 3 ml of organic solvent, namely hexane. After that, the mixture was put in an Ultra Sonic Bath in 40 °C for 15 min. This process helped extract VFAs and transfer them to the organic solvent. At the end of this process, the first 3 ml of supernatant of the tube were collected and placed in a distillation column. After distillation the liquid obtained was filtered with 0.45 μm filters and was ready for measurement in a gas chromatograph. This procedure was done for all samples. The efficiency of the extraction method was evaluated using the CRM46975 Supelco Volatile Free Acid Mix as a standard. The recovery efficiency was determined to be 59.6 ± 0.2%. The filtering was followed by the measurement of the concentrations of VFAs in a Shimadzu *Nexus* 2030 GC-BID plasma gas chromatograph. For their measurement the column was used an Agilent J&W HP-FFAP. More specifically, the method used for the estimation of concentration of VFAs follows. The method parameters consisted of a 1 μL sample injection volume, an injection temperature of 160 °C, an oven temperature program spanning from 80 °C to 230 °C, a flow rate of 59 mL/min, and a BID detector temperature set at 280 °C. The program for measuring VFAs had a duration of 21 min [49].

The next stage of the analysis focused on determining the concentration of FAMEs. This required a transesterification process, which was carried out in several steps. Initially, 200 μL of the sample was combined with 4 mL of a 0.5 M methanolic-KOH solution. The mixture was then heated to 80 °C for 15 min, with two stirring intervals. Following this, 1.6 mL of an HCl (4:1) solution was added, and the mixture was further heated to 80 °C for 25 min. Once the heating was complete, the mixture was allowed to cool, and 8 mL of deionized water was introduced. Subsequently, 15 mL of hexane was added to extract the FAMEs, leading to phase separation. The upper layer, containing hexane and FAMEs, was collected, and the liquid was filtered using a 0.45 μm filter. Additionally, 2 g of anhydrous sodium sulfate were placed at the end of the syringe to absorb any residual moisture. FAMEs were analyzed using the same plasma gas chromatograph (Shimadzu *Nexus* 2030 GC-BID) employed for VFAs, utilizing a MEGA 10 column. The method parameters included a 1 μL sample injection volume, an injection temperature of 240 °C, an oven temperature program ranging from 40 °C to 230 °C, a flow rate of 66.5 mL/min, and a BID detector temperature of 240 °C. The program for measuring FAMEs had a duration of 59 min [45].

2.2. Mass balances and statistical analysis

To determine the mass balances during HTL, the masses or volumes of all inputs (feedstock, process water, purge gas) and of each product phase (bio-crude, hydrochar, aqueous phase, non-condensable gas) were recorded with calibrated analytical balances (±0.01 g) and burettes (±0.5 mL). A one-way analysis of variance (ANOVA) was then carried out—separately for each temperature block—to test the effect of the four initial-pressure regimes (NoP, N_2, CO_2, N_2/ CO_2) on the response variables (phase yields, COD, HHV, VFA and FAME concentrations). All twelve operating conditions were sampled triplicates (technical replication). Statistical significance was accepted at the 95% confidence level ($p < 0.05$), and results are reported throughout the paper as mean ± standard deviation ($n = 3$). This approach captures run-to-run variability, ensures the validity of parametric tests and provides a transparent basis for comparing the influence of pressure on all measured HTL outputs.

2.3. Limitations of the study and future work

This work provides the first evidence that CO_2-pressurised HTL can enhance carboxylation pathways toward high-value fatty acids, yet several knowledge gaps remain that we intend to close in follow-up studies. The process scale-up and sustainability is one aspect since although report mass and energy yields are reported, a full techno-economic or life-cycle assessment was not carried out. In respect of the hydrochar products characterization, the higher HHV of the hydrochar was assessed, but a full detailed elemental, ash and surface analyses (XRD, SEM, BET) will be carried in a follow-up study. Likewise, we did not run gas-chromatography on the evolved gases, leaving the distribution of CO, H_2, CH_4 and light hydrocarbons unresolved. It is important to emphasize that the study focused on the effect of additional gases on the solid and liquid products of the process rather than on gaseous products and aqueous products. Specifically, exclusively focused on hydrochar and biocrude. The gaseous products were collected for a clearer picture of the mass yield of products. Anise waste served as a convenient single substrate, but comparative trials on other lignocellulosic biomass samples, algae and mixed food wastes are essential to confirm the generality of the CO_2 effect. Finally, while statistical links between pressure and product profiles are highlighted, kinetic modelling and isotope tracing are still required to fully describe the CO_2-driven carboxylation network. Future studies will therefore include detailed gas-phase GC analysis, in-depth hydrochar characterization, and the examination of a broader feedstock matrix. Finally, a comprehensive technoeconomic assessment and a life-cycle assessment will be performed.

3. Results and discussion

Regarding the mass balances of the products from hydrothermal liquefaction in a more generic context, Fig. 1 shows that in all samples that the largest amount appeared in bio-crude oil with a percentage ranging from 51% to 83%. The solid product (hydrochar) appeared to have increased from 310 °C to 350 °C while at 390 °C it decreased. In 310 °C and 350 °C the percentage of hydrochar was from 12% − 21% while in 390 °C the percentage fell and was from 4% to 6%. Gaseous products appeared in higher quantities at temperatures of 350 °C and 390 °C. Their percentages in this temperature range fluctuated from 18% − 43% and to 310 °C from 1% to 23%. More specifically, at 310 °C it was shown that bio-crude oil was reduced by the addition of gases and mainly by the presence of CO_2. On the other hand, the addition of CO_2 showed an increase in the quantities of hydrochar and gaseous products. At 350 °C in the cases of $S350N_2CO_2$ and $S350CO_2$ the presence of CO_2 showed an increase in the quantities of bio-crude oil and hydrochar but a decrease in gaseous products. Still at 390 °C the gaseous products decreased, more in the case of adding 10 bar N_2 than in the cases of 9 bar N_2 & 1 bar CO_2 and 1 bar CO_2. Regarding the quantities of hydrochar and bio-crude oil there was an increase compared to the S390NoP sample. In other words, CO_2 seems to have an effect on products at all temperatures. At 310 °C it increases hydrochar and gaseous products, at 350 °C it contributes to the increase of hydrochar and bio-crude oil, while at 390 °C it has a similar effect to 350 °C. In a more general context, hydrothermal liquefaction of biomass shows a yield of bio-crude oil at 10–60 wt% and in some cases reaches 80 wt%. Specifically, from woody biomass yields range from 20 to 30%, from algae the yield is about 45%, while from waste such as sewage sludge the yield of bio-crude oil ranges from 35 to 45% [50].

Fig. 2 highlights that the pH in the liquid product of hydrothermal liquefaction in all cases is in the alkaline range. At 310 °C it ranged from 7.3 to 7.8 and the largest value was in the $S310CO_2P$ sample. At 350 °C the pH values were from 7.5 to 7.8 and the largest appeared in the sample $S350N_2P$. On the other hand, at the temperature of 390 °C the pH was in the range of 7.7 to 8 while the highest value was in the sample s390NoP. It was generally observed that with an increasing temperature the pH value increased but without a rapid change. Correspondingly an increase in pH was observed in hydrothermal liquefaction experiments of Nannocloropsis sp. in temperature range of 250 °C to 350 °C and the

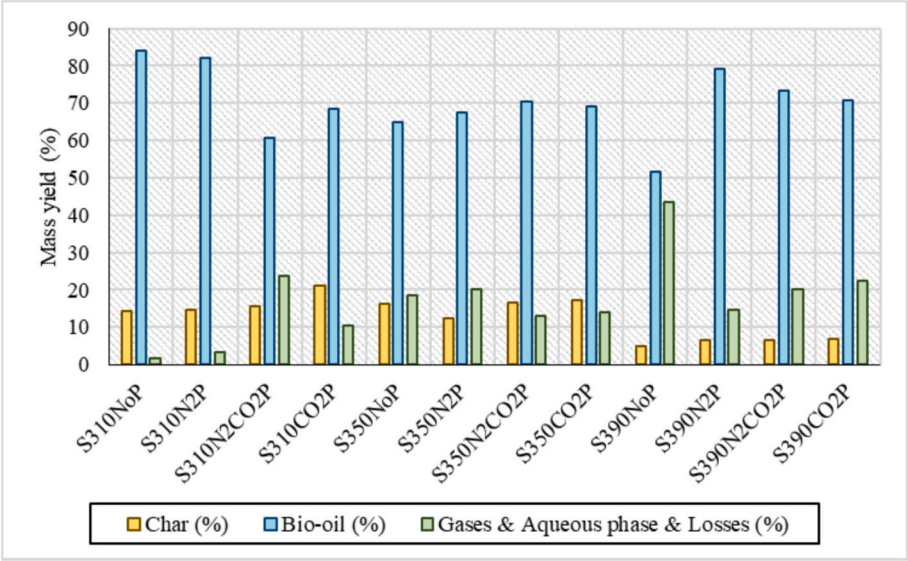

Fig. 1. Mass yield of hydrothermal liquefaction products.

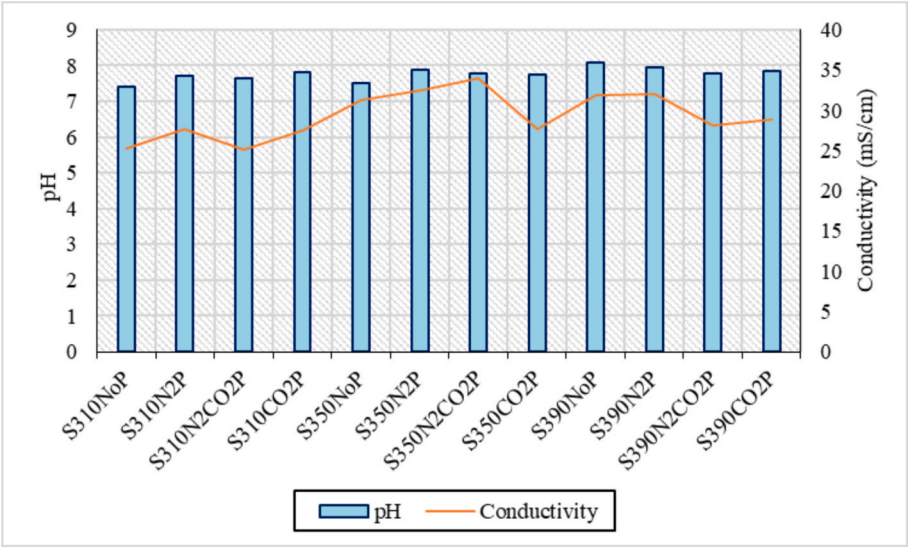

Fig. 2. Ph and conductivity analysis in aqueous phase.

pH values from 6.88 increased to 7.62 according to Hu et al. [51]. Still according to Yang et al. [52], hydrothermal liquefaction at 350 degrees of microalgae Tetraselcuis sp. it showed an alkaline pH of 8.88. These small increases are likely to have resulted from conversion of organic acids into alcohols through reduction at higher temperatures [40]. On the other hand, alkaline pH conditions contribute to the production of carboxylic acids in biocrude oil and specifically C2-C5 compounds [53].

The conductivity (mS/cm) of the samples was influenced by temperature and pressure. At 310 °C, conductivity was around 25 mS/cm for S310NoP and S310N_2CO_2P but increased to 27.6 and 27.5 mS/cm when N_2 and CO_2 were introduced separately. At 350 °C, conductivity increased across all pressurized conditions, with S350N_2CO_2P showing the highest value, 33.9 mS/cm, followed by S350N_2P, 32.4 mS/cm and S350NoP at 31.2 mS/cm. The lowest value at 27.7 mS/cm was observed in S350CO_2P, which remained like 310 °C counterpart. At 390 °C, S390NoP and S390N_2P exhibited conductivity around 32 mS/cm, while S390N_2CO_2P and S390CO_2P showed lower values (~28 mS/cm). Overall, conductivity peaked at 350 °C under N_2 and CO_2 pressure (S350N_2CO_2P at 33.9 mS/cm), with notable increases at 350 °C and 390 °C when N_2 and NoP were introduced.

Fig. 3 illustrates the concentration of COD. At 310 °C, COD values were relatively high, with S310NoP at 47,512 mg/L, S310N_2CO_2P at 57,832 mg/L, and S310CO_2 at 62,992 mg/L, except for the S310N_2P sample, which had the lowest value in its group. At 350 °C, a linear increase was observed, ranging from the lowest value in S350NoP at 21,486 mg/L to the highest in S350CO_2P at 45,538 mg/L. In contrast, at 390 °C, COD values showed less variation, with the lowest recorded in S390N_2CO_2P at 28,340 mg/L and the highest in S390N_2P at 36,036 mg/L. It was observed that under no-pressure conditions (NoP), COD concentration initially peaked at 310 °C, dropped significantly at 350 °C, and then increased slightly at 390 °C. The addition of N_2 had a positive effect, leading to higher COD values at 390 °C, while the values remained nearly unchanged at the other two temperatures. In experiments with N_2 and CO_2, COD was notably high at 310 °C, followed by a decline at the next two temperatures. Compared to other biomass species, in sorghum bagasse hydrothermal liquefaction experiments conducted in a temperature range of 300 °C to 350 °C COD concentrations ranged from 20,000–26,000 mg/L [54]. Also, according to Qian et al

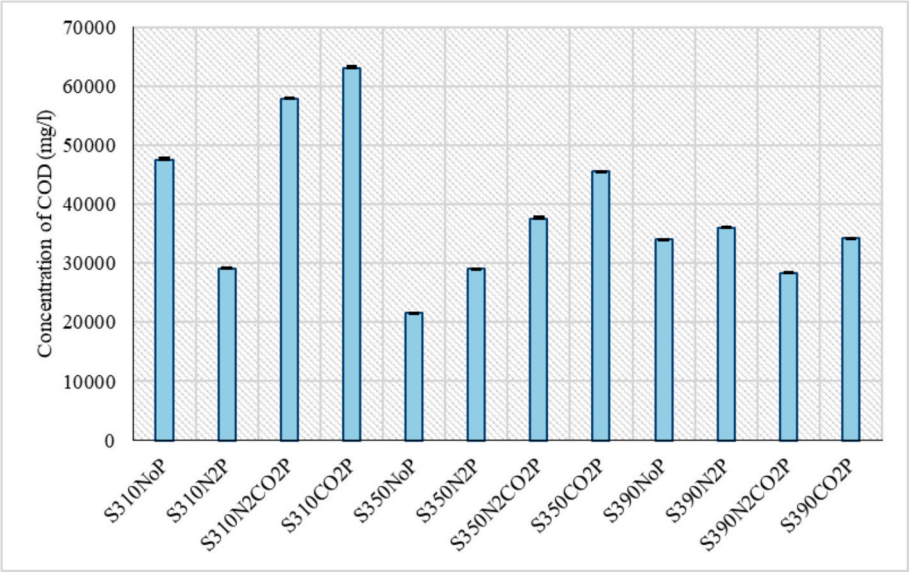

Fig. 3. COD measurements for all samples in aqueous phase.

[55], after experiments of hydrothermal liquefaction of *Chlorella* the concentration of COD was 38,520 mg/L. On the other hand, compared to non-lignocellulosic biomass, from sewage sludge hydrothermal liquefaction experiments at 325 °C the COD emerged to be 28,300 mg/L [56]. Finally, the addition of CO_2 resulted in relatively high COD values across all conditions, though there was a significant difference between the temperatures, with S310CO_2 at 62,992 mg/L, S350CO_2P at 45,538 mg/L, and S390CO_2P at 34,254 mg/L, revealing enrichment of the liquid product with organic products.

In Fig. 4, the concentrations of total phenols in the samples are measured using a spectrophotometer. The highest phenol content was observed in sample S390NoP at 3,095 mg/L, followed by S350N_2P at 2,348 mg/L, with a significant difference between them. The third-highest value was found in S310N_2CO_2P at 2,052 mg/L, while the lowest phenol concentration was recorded in S350N_2CO_2P at 950.5 mg/L. At 310 °C, the highest phenol production appeared to be promoted by the addition of both gases (N_2 and CO_2). At 350 °C, only nitrogen addition led to increased phenol levels, while at 390 °C, the highest concentration was found in the sample without any added gas (S390NoP). Regarding the impact of the added gases at each temperature, at 310 °C, there was an increase of approximately 200–500 mg/L with the addition of N_2 and N_2 & CO_2, while CO_2 addition resulted in a decrease of about 300 mg/L compared to the initial NoP value. Similarly, at 350 °C, nitrogen introduction led to an increase of approximately 500 mg/L, followed by a significant drop of 100–300 mg/L in the other two pressurized conditions. Finally, at 390 °C, the highest phenol concentration was observed under NoP conditions, while the other three samples showed no significant variation in their phenol levels. Generally, the addition of CO_2 seemed to act negatively on the production of phenols and prevent their formation for all samples. This reduction of phenols in the presence of CO_2 may be explained by the possibility of the gas helping to enhance bio-crude oil and hydrochar as according to Liu et al. [57], at higher temperatures through recombination reactions of phenolic compounds form light polyaromatic hydrocarbons in bio-crude oil and heavier ones forming hydrochar. This fact becomes intense at 390 °C where the presence of CO_2 increases the yield of bio-crude oil and hydrochar, in conditions that mainly favor the production of gas products.

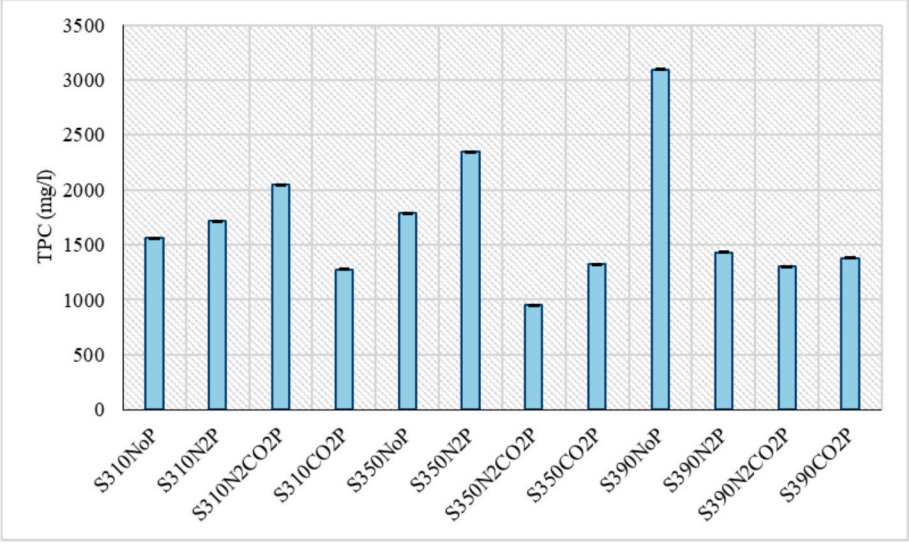

Fig. 4. Total phenols concentration of all samples.

It is observed at Fig. 5 that the HHV did not show significant variations across the samples at 310 °C and 350 °C, with a slight increase at 350 °C. For each temperature, the values remained nearly the same, with only minor decimal fluctuations. At 310 °C, HHV ranged around 33 MJ/kg (33.3–33.5 MJ/kg), while at 350 °C, it increased to 35 MJ/kg (35.1–35.9 MJ/kg). At 390 °C, a decrease in HHV was observed, with the lowest value recorded in sample S390NoP at 23.72 MJ/kg, followed by $S390N_2CO_2P$ at 26.04 MJ/kg. The other two samples showed values ranging between 27.4 and 27.5 MJ/kg. This reduction of the HHV at 390 °C can be attributed to the carboxylation reactions that take place most intensively at temperatures 300–350 °C and produce carboxylic volatile fatty acids and carboxylic fatty acids with high energy content, like stearic acid, palmitic acid and arachidic acid [49]. In general, it was observed in all cases that the presence of CO_2 affected the high heating value of hydrochar, giving an increase in the HHV of hydrochar. Compared to other raw materials according to Zhang et al. [58], hydrochar from corn cob from hydrothermal liquefaction at 310 °C, residence time 1.5 h had HHV of 26.6 MJ/Kg and respectively at 370 °C had HHV of 27.6 MJ/Kg. Also, from hydrothermal liquefaction of canola straw at 300 °C and a residence time of 4 h, hydrochar with a HHV of 29.6 MJ/Kg was obtained [59]. Furthermore, hydrochar produced by hydrothermal liquefaction of vineyard waste at 300 °C with a residence time of 1 h had a HHV of 25.4 MJ/Kg and respectively at 350 °C, hydrochar with a HHV of 28.4 MJ/Kg emerged [58].

As presented in Fig. 6, the VFAs recorded from the analyses conducted on the samples are illustrated. The only acid that appeared in all the samples, and had the highest concentrations found in the diagram, was Acetic Acid in the samples $S310CO_2P$, $S310N_2CO_2P$, and S350NoP, in descending order. In the other samples, the concentration of Acetic Acid ranged from approximately 16.5 mg/L to 38.3 mg/L. In all samples, except for $S310N_2P$, Formic Acid, also known as Methanoic Acid, was detected in much lower quantities, though it remained at nearly the same levels across all the samples, ranging from 27.5 to 31.1 mg/L. Isovaleric Acid showed zero concentration in the samples S310NoP, $S310N_2P$, $S350N_2P$, and S390NoP, while Valeric Acid was found in very small concentrations, specifically 1.43 mg/L and 1.83 mg/L, only in the samples $S390N_2P$ and $S390N_2CO_2P$, and was absent in all other samples. The sample $S310N_2P$ had the lowest VFA production when compared to the other samples. In hydrothermal liquefaction experiments of cornstalk at 375 °C Acetic Acid formed the most prevalent compound and ranged from 24% to 36% [60]. In addition, according to Panisco et al. [61] in hydrothermal liquefaction experiments at 350 °C from corn stover Acetic Acid was 20% of the total carbon, Formic Acid made up 1% and Propionic acid 2% of the total carbon. The general trend indicated by the Diagram led to the conclusion that the addition of N_2 did not improve VFAs production, while the addition of CO_2 and the combination of both gases were beneficial for VFAs production. Additionally, the 390 °C temperature showed an increase in VFAs compared to the previous two temperatures, except for the samples with the highest concentrations.

In Fig. 7, the Fatty Acid Methyl Esters are presented. FAMEs are inextricably linked to the quality of bio-crude oil and their physicochemical characteristics have a large impact on the combustion and performance of bio-crude [62]. The general trend observed in the Figure was an upward increase in FAMEs as the temperature of the experiments increased, except for the sample S310NoP, which had higher concentrations than the other samples at the same temperature. The overall concentration detected was equal to that of the sample $S350N_2CO_2P$. The latter also had the highest concentration of Methyl Esters in the temperature group it was in. The highest production was detected at 390 °C, specifically in the samples $S390N_2CO_2P$, $S390CO_2P$, and $S390N_2P$, in descending order. Regarding the comparison between samples at each temperature, at 310 °C, the sample S310NoP had the highest FAME production, with Methyl stearate having the largest concentration in the sample, 5,159.8131 mg/L. A relatively high concentration of FAMEs was observed in the sample $S310N_2CO_2P$, with the methyl ester Methyl hexanoate showing the largest concentration in the sample, 1,527.505 mg/L. At 350 °C, the sample S350NoP had the lowest FAME production, while the other three showed no significant deviations from each other. Finally, at 390 °C, it appeared that the conditions without pressure did not favor the production of Methyl Esters, as the lowest concentrations in the group were recorded. The addition of the gases individually favored production but not as drastically as when both gases were applied simultaneously, as seen in the case of the sample $S390N_2CO_2P$. This specific sample contained the highest possible number of produced FAMEs, specifically Methyl hexanoate, 13,132.153 mg/L, Methyl octanoate, 11,925.32 mg/L, Methyl linoleate, *cis*-9,12, 6,088.186 mg/L, and Methyl butyrate, 3,470.3864 mg/L. The other two samples at this temperature had high concentrations relative to the other samples, with $S390N_2P$ having the second highest concentration of the Methyl hexanoate ester, 8,578.945 mg/L. In hydrothermal liquefaction experiments food waste produced 15–37 wt% of bio-crude oil content with the most widespread being FAMEs C16-C18 and specifically palmitic acid, palmitoleic acid, stearic acid [63]. Also, according to Brown et al. [64] in hydrothermal liquefaction experiments of Nannocloropsis sp. at 350 °C the main FAMEs that appeared in bio-crude oil were from

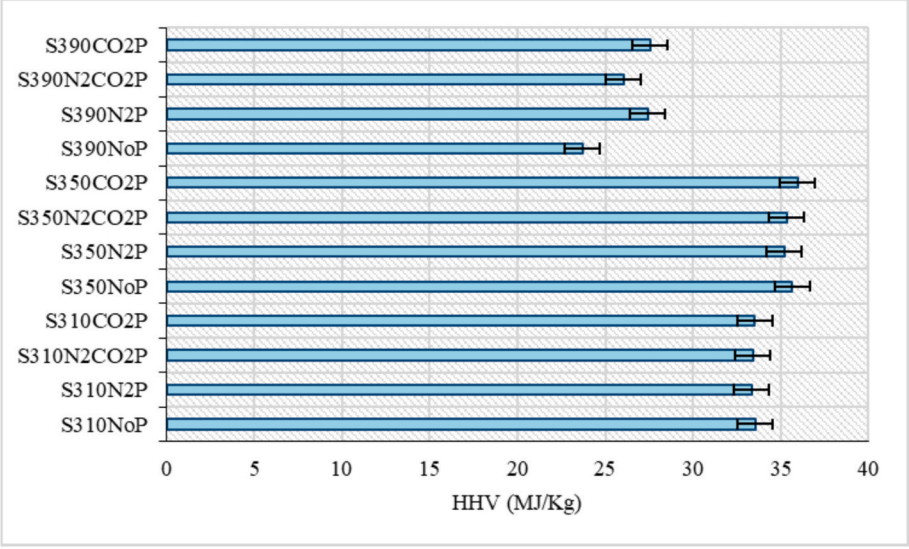

Fig. 5. High Heating Value of hydrochar.

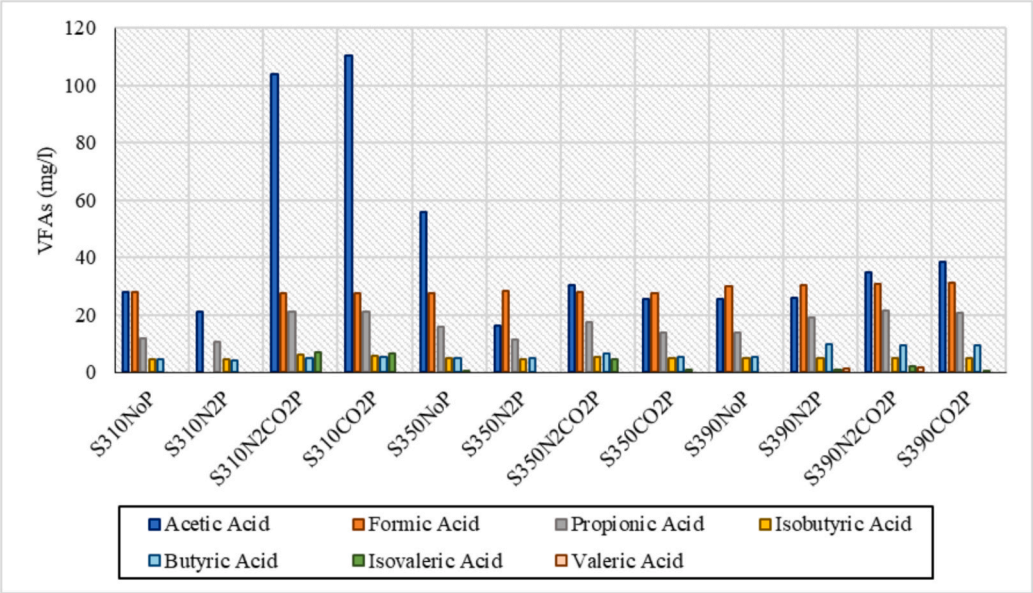

Fig. 6. Concentration of Volatile Fatty Acids.

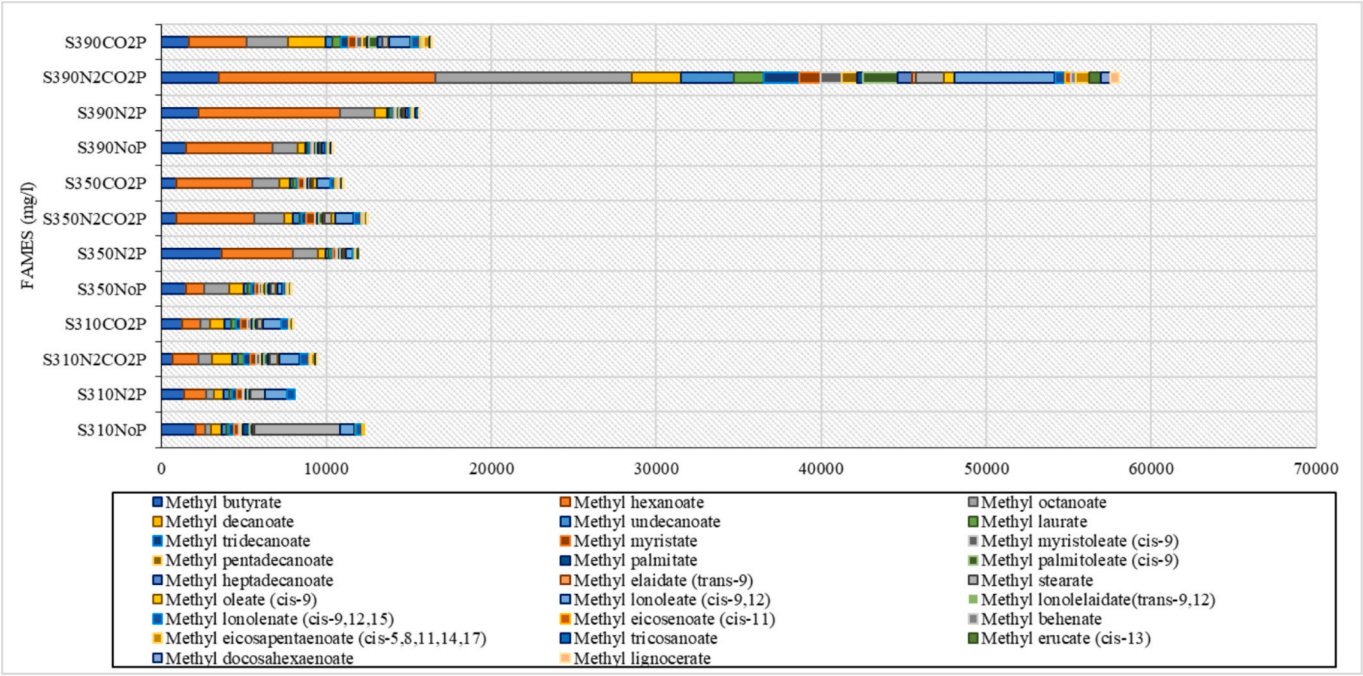

Fig. 7. Concentration of FAMEs in biocrude oil.

C14-C20 and specifically eicosapentaenoic acid, palmitoleic acid, palmitic acid, myristic acid, arachidonic acid, oleic acid and linoleic acid. Overall, it was noted that as the reaction temperature increased, the addition of CO_2 enhanced FAMEs production. A similar trend was observed in the samples where both gases (N_2 and CO_2) were introduced.

A one-way ANOVA statistical analysis was conducted to examine the effect of different pressure levels on the production of VFAs. The results in Table 2 showed that pressure variations significantly influence VFA production. Specifically, for every tested temperature, the p-value was found to be less than 0.05, indicating that the differences in pressure conditions are statistically significant. This suggests that pressure is a key factor affecting the production process of VFAs, meaning that changes in pressure can lead to notable variations in VFA yield. These findings highlight the importance of optimizing pressure conditions to enhance VFA production efficiency.

The results indicate that different pressure conditions influence the formation of FAMEs. One-way ANOVA analysis in Table 3 showed that pressure had a statistically significant effect at 310 °C and 350 °C. However, at 390 °C, the p-value did not indicate a significant difference, suggesting that pressure may have a less pronounced impact at higher temperatures. This could be attributed to the fact that FAMEs may form through multiple thermochemical pathways, potentially reducing the direct influence of pressure on their overall yield. In contrast, the effect of pressure may be more distinct in the case of VFAs, as their formation is likely governed by more specific reaction mechanisms that are more

Table 2
One-way ANOVA for VFAs.

Source of Variation	SS	df	MS	F	p-value	F crit
The pressure factor in concentrations of VFAs: 310 °C						
Between the groups	10172,4	4	2543,1	5,035944	0,008933	3,055568
Inside the groups	7574,848	15	504,9898			
Total	17747,25	19				
The pressure factor in concentrations of VFAs: 350 °C						
Between the groups	2523,37	4	630,8426	10,8091	0,000251	3,055568
Inside the groups	875,4324	15	58,36216			
Total	3398,803	19				
The pressure factor in concentrations of VFAs: 390 °C						
Between the groups	2360,577	4	590,1443	49,53147	1,81E-08	3,055568
Inside the groups	178,718	15	11,91453			
Total	2539,295	19				

Table 3
One-way ANOVA of FAMEs.

Source of variation	SS	df	MS	F	p-value	F crit
The pressure factor in concentrations of FAMEs: 310 °C						
Between the groups	11319370,78	10	1131937,078	2,246	0,039443313	2,132
Inside the groups	16628781,18	33	503902,4601			
Total	27948151,97	43				
The pressure factor in concentrations of FAMEs: 350 °C						
Between the groups	1252975,712	10	125297,5712	6,022	3,85931E-05	2,132
Inside the groups	686525,3705	33	20803,79911			
Total	1939501,082	43				
The pressure factor in concentrations of FAMEs: 390 °C						
Between the groups	10690491,38	10	1069049,138	1,136	0,366068457	2,132
Inside the groups	31033470,79	33	940408,2056			
Total	41723962,17	43				

sensitive to pressure variations. Future studies should further investigate these effects, particularly by analyzing the dominant reaction pathways at different temperature and pressure conditions to better understand their role in biofuel production.

4. Conclusion

This work shows that the atmospheric mix in the reactor during hydrothermal liquefaction has a decisive effect on product quality and yield. Elevated temperatures (350–390 °C) favored the formation of both VFAs and FAMEs, but product selectivity depended strongly on the pressure and gas atmosphere. The addition of N_2 alone did not improve VFA production, whereas CO_2 and N_2/CO_2 atmospheres dramatically enhanced carboxylation reactions and resulted in higher concentrations of acetic acid, methyl hexanoate and other FAMEs. At 390 °C the combination of N_2 and CO_2 produced up to 13 g/ L methyl hexanoate and 11.9 g/ L methyl octanoate. On the one hand, CO_2 also improved hydrochar quality and the higher heating value reached 35 MJ/ kg at 350 °C but declined at 390 °C in the absence of gas. On the other hand, CO_2 pressurization mitigated this decrease. The presence of CO_2 suppressed phenol formation, suggesting that the gas promoted recombination of phenolic intermediates into heavier hydrocarbons and enhanced carbon retention in hydrochar. One-way ANOVA confirmed that pressure significantly affected VFA and FAME yields at 310–350 °C but not at 390 °C, implying that multiple thermochemical pathways operate at higher temperatures. Overall, reactive CO_2 atmospheres shift the HTL chemistry towards carboxylated products and high-value fatty-acid esters. Optimizing the feed gas composition and total pressure is therefore a promising lever for producing tailored biocrudes and hydrochars from wet biomass residues.

Declaration of generative AI and AI-assisted technologies in the writing process

During the preparation of this work the author(s) used ChatGPT 4o in order to improve language and readability, with caution. After using this tool/service, the author(s) reviewed and edited the content as needed and take full responsibility for the content of the publication.

CRediT authorship contribution statement

D. Liakos: Writing – original draft, Visualization, Investigation, Formal analysis, Data curation. **Maria Iosifidou:** Investigation, Formal analysis, Data curation. **S. Vakalis:** Writing – review & editing, Writing – original draft, Validation, Supervision, Resources, Project administration, Methodology, Investigation, Funding acquisition, Data curation, Conceptualization.

Declaration of competing interest

The authors declare that they have no known competing financial interests or personal relationships that could have appeared to influence the work reported in this paper.

Acknowledgements

The research was partially funded by the project BioFairNet, which has received funding from the European Commission's Horizon Europe research and innovation program under Grant Agreement No 101181568.

Data availability

Data will be made available on request.

References

[1] Saengsuriwong R, Onsree T, Phromphithak S, Tippayawong N. Biocrude oil production via hydrothermal liquefaction of food waste in a simplified high–throughput reactor. Bioresour Technol 2021;341:125750.

[2] Aierzhati A, Stablein MJ, Wu NE, Kuo CT, Si B, Kang X, et al. Experimental and model enhancement of food waste hydrothermal liquefaction with combined effects of biochemical composition and reaction conditions. Bioresour Technol 2019;284:139–47.
[3] Schanes K, Dobernig K, Gözet B. Food waste matters – a systematic review of household food waste practices and their policy implications. J Clean Prod 2018; 182:978–91.
[4] Vigano J, da Fonseca Machado AP, Martinez J. Sub– and supercritical fluid technology applied to food waste processing. J Supercrit Fluids 2015;96:272–86.
[5] Pham TPT, Kaushik R, Parshetti GK, Mahmood R, Balasubramanian R. Food waste–to–energy conversion technologies: current status and future directions. Waste Manag 2015;38:399–408.
[6] Walia B, Sanders S. Curbing food waste: a review of recent policy and action in the USA. Renew Agric Food Syst 2019;34:169–77.
[7] Mourad M. Recycling, recovering and preventing "food waste": competing solutions for food systems sustainability in the United States and France. J Clean Prod 2016;126:461–77.
[8] Skaggs RL, Coleman AM, Seiple TE, Milbrandt AR. Waste–to–energy biofuel production potential for selected feedstocks in the conterminous United States. Renew Sustain Energy Rev 2018;82:2640–51.
[9] Motavaf B, Savage PE. Effect of process variables on food waste valorization via hydrothermal liquefaction. ACS ES&T Eng 2021;1:363–74.
[10] Teigiserova DA, Hamelin L, Thomsen M. Towards transparent valorization of food surplus, waste and loss: clarifying definitions, food waste hierarchy, and role in the circular economy. Sci Total Environ 2020;706:136033.
[11] Anli RE, Bayram M. Traditional aniseed–flavored spirit drinks. Food Rev Int 2010; 26:246–69.
[12] Sun W, Shahrajabian MH, Cheng Q. Anise (*Pimpinella anisum* L.), a dominant spice and traditional medicinal herb for both food and medicinal purposes. Cogent Biol 2019;5:1673688.
[13] Carmichael SW, Oshel P. Why is my ouzo cloudy? Microsc Today 2023;31:8–9.
[14] Vendramin V, Pesce A, Vincenzi S. Anethole stability in aniseed spirits: storage condition repercussions on commercial products. Beverages 2021;7:73.
[15] Sharafan M, Jafernik K, Ekiert H, Kubica P, Kocjan R, Blicharska E, et al. *Illicium verum* (Star Anise) and trans–anethole as valuable raw materials for medicinal and cosmetic applications. Molecules 2022;27:650.
[16] Kontominas MG. Volatile constituents of Greek ouzo. J Agric Food Chem 1986;34: 847–89.
[17] Anastasopoulou E, Graikou K, Ganos C, Calapai G, Chinou I. *Pimpinella anisum* seeds essential oil from Lesvos island: effect of hydrodistillation time, comparison of its aromatic profile with other samples of the Greek market. Safe use Food and Chemical Toxicology 2020;135:110875.
[18] Gökşen G, Ekiz HI. Use of aniseed cold-pressed by-product as a food ingredient in muffin formulation. LWT 2021;148:111722.
[19] Karapanagioti HK, Bekatorou A. Alcohol and dilution water characteristics in distilled anis (Ouzo). J Agric Food Chem 2014;62:4932–14497.
[20] Tekin K, Karagöz S, Bektaş S. A review of hydrothermal biomass processing. Renew Sustain Energy Rev 2014;40:673–87.
[21] Xue Y, Chen H, Zhao W, Yang C, Ma P, Han S. Operating conditions of producing bio–oil from hydrothermal liquefaction of biomass. Int J Energy Res 2016;40: 865–77.
[22] Aktas K, Liu H, Eskicioglu C. Treatment of aqueous phase from hydrothermal liquefaction of municipal sludge by adsorption: comparison of biochar, hydrochar, and granular activated carbon. J Environ Manag 2024;356:120619.
[23] Toor SS, Rosendahl L, Rudolf A. Hydrothermal liquefaction of biomass: a review of subcritical water technologies. Energy 2011;36(5):2328–42.
[24] Sandquist J, Tschentscher R, del Alamo Serrano G. Hydrothermal liquefaction of organic resources in biotechnology: how does it work and what can be achieved? Appl Microbiol Biotechnol 2019;103(2):673–84.
[25] Mathanker A, Das S, Pudasainee D, Khan M, Kumar A, Gupta R. Hydrothermal liquefaction of biomass for biofuels production with a special focus on the effect of process parameters, co–solvents and extraction solvents. Energies 2021;14:4916.
[26] Beims RF, Hu Y, Shui H, Xu CC. Hydrothermal liquefaction of biomass to fuels and value-added chemicals: Products applications and challenges to develop large-scale operations. Biomass Bioenergy 2020;135:105510.
[27] Gollakota ARK, Kishore N, Gu S. A review on hydrothermal liquefaction of biomass. Renew Sustain Energy Rev 2018;81:1378–92.
[28] Vardon DR, Sharma BK, Scott J, Yu G, Wang Z, Schideman L, et al. Chemical properties of biocrude oil from the hydrothermal liquefaction of Spirulina algae, swine manure and digested anaerobic sludge. Bioresour Technol 2011;102: 8295–303.
[29] Shanmugam SR, Adhikari S, Wang Z, Shakya R. Treatment of aqueous phase of bio–oil by granular activated carbon and evaluation of biogas production. Bioresour Technol 2017;223:115–20.
[30] Shafizadeh A, Shahbeig H, Nadian MH, Mobli H, Dowlati M, Gupta VK, et al. Machine learning predicts and optimises hydrothermal liquefaction of biomass. Chem Eng J 2022;445:136579.
[31] Raikova S, Le CD, Wagner JL, Ting VP, Chuck CJ. Towards an aviation fuel through the hydrothermal liquefaction of algae. In: Chuck CJ, editor. Biofuels for Aviation. London: Academic Press; 2016. p. 217–39.
[32] Lozano EM, Pedersen TH, Rosendahl LA. Modelling of thermochemically liquefied biomass products and heat of formation for process energy assessment. Appl Energy 2019;254:113654.
[33] Hao B, Xu D, Jiang G, Sabri TA, Jing Z, Guo Y. Chemical reactions in the hydrothermal liquefaction of biomass and in the catalytic hydrogenation upgrading of biocrude. Green Chem 2021;23:1562–83.
[34] Amaniampong PN, Asiedu NY, Fletcher E, Dodoo–Arhin D, Olatunji OJ, Trinh QT. Conversion of lignocellulosic biomass to fuels and value–added chemicals using emerging technologies and density functional theory simulations. In: Valorization of Biomass to Value–Added Commodities: Current Trends, Challenges, and Future Prospects. 2020:193–220.
[35] Yang J, Niu H, Corscadden K, Astatkie T. Hydrothermal liquefaction of biomass model components for product yield prediction and reaction pathways exploration. Appl Energy 2018;228:1618–28.
[36] Aida TM, Shiraishi N, Kubo M, Watanabe M, Smith Jr RL. Reaction kinetics of d–xylose in sub– and supercritical water. J Supercrit Fluids 2010;55:208–16.
[37] Sato N, Quitain AT, Kang K, Daimon H, Fujie K. Reaction kinetics of amino acid decomposition in high–temperature and high–pressure water. Ind Eng Chem Res 2004;43:3217–22.
[38] Gai C, Zhang Y, Chen WT, Zhang P, Dong Y. Reaction pathways of hydrothermal liquefaction using Chlorella pyrenoidosa and Spirulina platensis. Energy Convers Manag 2015;96:330–9.
[39] Sohn M, Ho CT. Ammonia generation during thermal degradation of amino acids. J Agric Food Chem 1995;43:3001–3.
[40] Watanabe M, Iida T, Inomata H. Decomposition of a long–chain saturated fatty acid with some additives in hot compressed water. Energy Convers Manag 2006;47: 3344–50.
[41] Biller P, Roth A. Hydrothermal liquefaction: a promising pathway towards renewable jet fuel. In: Chuck CJ, editor. Biokerosene: Status and Prospects. 2018. p. 607–35.
[42] Chen Z, Rao Y, Usman M, Chen H, Białowiec A, Zhang S, et al. Anaerobic fermentation of hydrothermal liquefaction wastewater of dewatered sewage sludge for volatile fatty acids production. Sci Total Environ 2021;777:146077.
[43] Vo TK, Kim SS, Ly HV, Lee EY, Lee CG, Kim J. Reaction network and kinetic model of the hydrothermal liquefaction of microalgae Tetraselmis sp. Bioresour Technol 2017;241:610–19. (ΠΑΛΙΟ 42).
[44] Rogalinski T, Liu K, Albrecht T, Brunner G. Hydrolysis kinetics of biopolymers in subcritical water. J Supercrit Fluids 2008;46:335–41.
[45] Liakos D, Altiparmaki G, Malamis S, Vakalis S. Hydrothermal liquefaction for biofuel synthesis: assessment of VFA and FAME profiles from spent coffee grounds. Energies 2025;18(8):2094.
[46] Sklavos S, Gatidou G, Stasinakis AS, Haralambopoulos D. Use of solar distillation for olive mill wastewater drying and recovery of polyphenolic compounds. J Environ Manag 2015;162:46–52.
[47] Apha. Standard methods for the examination of water and wastewater. 20th ed. Baltimore, MD: American Public Health Association; 1998.
[48] Altiparmaki G, Kourletakis P, Moustakas K, Vakalis S. Assessing the effect of hydrothermal treatment (HT) severity on the fate of nitrates and phosphates in dairy wastewater. Fuel 2022;312:122866.
[49] Liakos D, Altiparmaki G, Moustakas K, Malamis S, Vakalis S. The fate of volatile fatty acids during the thermodynamic transition from hydrothermal carbonization to hydrothermal liquefaction: HTC-to-HTL. Sustain Chem Pharm 2024;41:101683.
[50] Dimitriadis A, Bezergianni S. Hydrothermal liquefaction of various biomass and waste feedstocks for biocrude production: a state–of–the–art review. Renew Sustain Energy Rev 2017;68:113–25.
[51] Hu Y, Gong M, Feng S, Xu CC, Bassi A. Recent developments of pre–treatment technologies and hydrothermal liquefaction of microalgae for bio–crude oil production. Renew Sustain Energy Rev 2019;101:476–92.
[52] Yang CM, Lee CG, Won JI. Improvement of bio–crude oil yield and phosphorus content by hydrothermal liquefaction using microalgae. Chem Eng Technol 2017; 40:2188–96.
[53] Feng S, Yuan Z, Leitch M, Xu CC. Hydrothermal liquefaction of barks into bio–crude – effects of species and ash content/composition. Fuel 2014;116:214–20.
[54] Bi Z, Zhang J, Peterson E, Zhu Z, Xia C, Liang Y, et al. Biocrude from pretreated sorghum bagasse through catalytic hydrothermal liquefaction. Fuel 2017;188: 112–20.
[55] Qian L, Ma X, Zhao S, Yuan C, Zhang B, Ding X, et al. Fast hydrothermal co-liquefaction of high-ash sludge and Chlorella for biocrude production. Algal Res 2024;82:103613.
[56] Thomsen LBS, Anastasakis K, Biller P. Wet oxidation of aqueous phase from hydrothermal liquefaction of sewage sludge. Water Res 2022;209:117863.
[57] Liu H, Basar IA, Lyczko N, Nzihou A, Eskicioglu C. Incorporating hydrothermal liquefaction into wastewater treatment – Part I: process optimisation for energy recovery and evaluation of product distribution. Chem Eng J 2022;449:137838.
[58] Zhang L, Wang Q, Wang B, Yang G, Lucia LA, Chen J. Hydrothermal carbonisation of corncob residues for hydrochar production. Energy Fuels 2015;29:872–86.
[59] Nzediegwu C, Naeth MA, Chang SX. Carbonisation temperature and feedstock type interactively affect chemical, fuel and surface properties of hydrochars. Bioresour Technol 2021;330:124976.
[60] Zhu Z, Si B, Lu J, Watson J, Zhang Y, Liu Z. Elemental migration and characterisation of products during hydrothermal liquefaction of cornstalk. Bioresour Technol 2017;243:9–16.
[61] Panisko E, Wietsma T, Lemmon T, Albrecht K, Howe D. Characterisation of the aqueous fractions from hydrotreatment and hydrothermal liquefaction of lignocellulosic feedstocks. Biomass Bioenergy 2015;74:162–71.
[62] Vimali E, Gunaseelan S, Devi VC, Mothil S, Arumugam M, Ashokkumar B, et al. Comparative study of different catalysts mediated FAME conversion from

macroalga Padina tetrastromatica biomass and hydrothermal liquefaction facilitated bio–oil production. Chemosphere 2022;292:133485.
[63] Bayat H, Dehghanizadeh M, Jarvis JM, Brewer CE, Jena U. Hydrothermal liquefaction of food waste: effect of process parameters on product yields and chemistry. Front Sustain Food Syst 2021;5:658592.
[64] Brown TM, Duan P, Savage PE. Hydrothermal liquefaction and gasification of Nannochloropsis sp. Energy Fuels 2010;24:3639–46.